

# Effects of surface-modifying ligands on the colloidal stability of ZnO nanoparticle dispersions in in vitro cytotoxicity test media

Dongwook Kwon  
Jonghoon Park  
Jaehong Park  
Seo Yeon Choi  
Tae Hyun Yoon

Laboratory of Nanoscale  
Characterization and Environmental  
Chemistry, Department of Chemistry,  
College of Natural Sciences, Hanyang  
University, Seoul, South Korea

**Abstract:** The extrinsic physicochemical properties of nanoparticles (NPs), such as hydrodynamic size, surface charge, surface functional group, and colloidal stabilities, in toxicity testing media are known to have a significant influence on in vitro toxicity assessments. Therefore, interpretation of nanotoxicity test results should be based on reliable characterization of the NPs' extrinsic properties in actual toxicity testing media. Here, we present a set of physicochemical characterization results for commercially available ZnO NPs, including core diameter, hydrodynamic diameter, surface charges, and colloidal stabilities, in two in vitro toxicity testing media (Roswell Park Memorial Institute [RPMI] and Dulbecco's Modified Eagle's Medium [DMEM]), as well as simple cell viability assay results for selected ZnO NPs. Four commercially available and manufactured ZnO NPs, with different core sizes, were used in this study, and their surface charge was modified with five different surface coating materials (sodium citrate, tris(2-aminoethyl)amine, poly(acrylic acid), poly(allylamine hydrochloride), and poly-L-lysine hydrochloride). The results showed that ZnO NPs were better dispersed in cell culture media via surface modification with positively or negatively charged molecules. Moreover, in the presence of fetal bovine serum (FBS) in RPMI and DMEM media, ZnO NPs were found even better dispersed for a longer period (at least 48 hours). For the HeLa cells exposed to ZnO NPs in DMEM media without FBS, surface charge-dependent cytotoxicity trends were observed, while these trends were not observed for those cells cultured in FBS-containing media. This confirmed the important roles of surface-modifying compounds and of surface charge on the resultant cytotoxicities of NPs.

**Keywords:** surface modification, agglomeration, sedimentation

## Introduction

Among various kinds of manufactured nanomaterials, ZnO nanoparticles (NPs) have been applied to a broad array of industrial products, including sunscreens, biosensors, food additives, pigments, rubber, and electronic materials.<sup>1,2</sup> Furthermore, due to their antibacterial activity, ZnO NPs have potential applications as prophylactic drugs against bacterially related infections and diseases.<sup>3</sup> Accordingly, the potential toxicity of ZnO NPs has been extensively studied, as documented in recent publications.<sup>4-6</sup>

According to recent nanotoxicological studies, the biological toxicity of NPs is closely related to many physicochemical properties, including particle size, shape, aggregation, and surface charge.<sup>7-10</sup> In human lung epithelial cells, smaller

Correspondence: Tae Hyun Yoon  
Laboratory of Nanoscale  
Characterization and Environmental  
Chemistry, Department of Chemistry,  
College of Natural Sciences,  
Hanyang University, 17 Haengdang-dong,  
Seongdong-gu, Seoul 133-791,  
South Korea  
Tel +82 2 2220 4593  
Fax +82 2 2299 0762  
Email [thyoon@gmail.com](mailto:thyoon@gmail.com)

ZnO NPs were reported to have greater toxicity than larger NPs and nanorod-shaped ZnO NPs were reported to be more toxic than spherical NPs, suggesting that both the size and shape of the NPs influence their cytotoxicity.<sup>11</sup> Morphological effects were also evaluated for toxicity to marine diatoms, and rod-shaped ZnO NPs were found to have greater toxicity than spherical NPs.<sup>12</sup> Additionally, a recent study on the effect of surface charge found that ZnO NPs preferentially attached to a negatively charged bacterial surface.<sup>13</sup> According to these studies, the toxicity of NPs was significantly influenced by their physicochemical properties. Therefore, it is important to understand correlations between biological toxicity and the physicochemical properties of NPs to develop an unbiased assessment of the potential risks of NPs.

Agglomeration and sedimentation are influenced by particle concentration, surface charge, shape of the NPs,<sup>14</sup> and the media composition. The presence of proteins or other small ligands in the media could also create dramatic variations of NP association.<sup>15</sup> The significant agglomeration and toxicity of NPs were observed in cell culture media without serum than with serum.<sup>16</sup> Thus the interpretation of nanotoxicity test results should be based on the reliable physicochemical characterization of NPs and their suspensions. Recently, the colloidal stability of NPs in toxicity test media has been studied. The hydrodynamic diameter of TiO<sub>2</sub> NPs was monitored in phosphate-buffered saline (PBS) and Dulbecco's Modified Eagle's Medium (DMEM).<sup>17</sup> The agglomeration and sedimentation of TiO<sub>2</sub> NPs were investigated in Roswell Park Memorial Institute (RPMI) medium with various concentrations of fetal bovine serum (FBS).<sup>18</sup> Furthermore, an optimized dispersion method was reported using various NPs (ie, Ag, ZnO, SiOx, and single and multi walled carbon nanotubes) for in vitro and in vivo toxicity testing.<sup>19</sup> These studies were needed to correlate observed biological effects with the physicochemical properties of NPs.

In this study, we present several sets of results of the physicochemical characterization of ZnO NPs suspended in toxicity test media. Four commercially available ZnO NPs with different core sizes were used, and their suspensions were prepared with five different surface coating materials (citrate, tris(2-aminoethyl)amine, poly(acrylic acid), poly(allylamine hydrochloride), and poly-L-lysine hydrochloride). We investigated the agglomeration and sedimentation behaviors of ZnO NPs in different cell culture media typically used for in vitro toxicity tests (ie, DMEM and RPMI). Temporal changes in the optical

densities (OD) and hydrodynamic size distributions were monitored using ultraviolet-visible (UV-Vis) spectroscopy and dynamic light scattering (DLS). In addition, the primary particle sizes, shapes, and surface charges were also measured.

## Materials and methods

### Preparation of ZnO NP dispersions

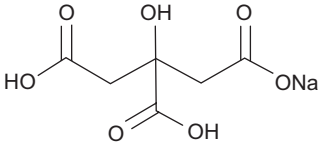
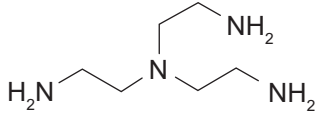
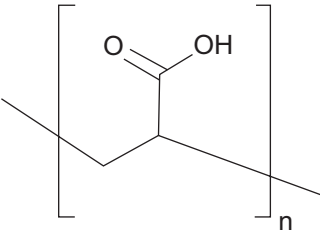
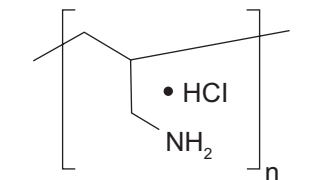
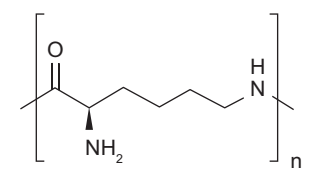
Four types of ZnO NPs were purchased from commercial sources: 20 nm ZnO (ZnO<sup>AA20</sup>) (Alfa Aesar, Ward Hill, MA, USA), 10–35 nm ZnO (ZnO<sup>SM20</sup>) (Sumitomo Osaka Cement Co., Ltd., Tokyo, Japan), 10–30 nm ZnO (ZnO<sup>AE20</sup>) (American Elements, Los Angeles, CA, USA), and <100 nm ZnO (ZnO<sup>AE100</sup>) (American Elements).

We prepared uncoated and also five different surface-coated ZnO NP suspensions. We used five coatings purchased from Sigma-Aldrich Corp (St Louis, MO, USA), sodium citrate, tris(2-aminoethyl)amine, poly(acrylic acid) (PAA), poly(allylamine hydrochloride) (PAH), and poly-L-lysine hydrochloride (PLL), respectively, to prepare sodium citrate-coated ZnO (ZnO<sup>(Cit)</sup>), tris(aminoethyl)amine-coated ZnO (ZnO<sup>(Tris)</sup>), PAA-coated ZnO (ZnO<sup>(PAA)</sup>), PAH-coated ZnO (ZnO<sup>(PAH)</sup>), and PLL-coated ZnO (ZnO<sup>(PLL)</sup>) (Table 1). The surface-coated ZnO NPs were prepared with the following method, described in detail in our recent publications:<sup>15</sup> Briefly, 4 g of ZnO NP powder was mixed with deionized water (DIW), 10 g/L sodium citrate or tris(aminoethyl)amine, or 5 g/L PAA, PAH, or PLL, to give 20 mL solutions, respectively. Before coating, the solutions were adjusted to approximately pH 7.0, using 0.1 M NaOH solution. Next, the ZnO solutions were sonicated for 60 minutes at 30 W (Ultrasonic cleaner, Daihan Scientific Co. Ltd., Seoul, Korea), and the dispersed ZnO solutions were prepared in the toxicity test medium, RPMI 1640 (Life Technologies Corp, Carlsbad, CA, USA) or DMEM (Welegene Inc., Daegu, Korea) with/without FBS (Life Technologies Corp).

### Characterization of ZnO NPs

The particle size and morphology of ZnO NPs were measured by transmission electron microscopy (TEM) (H-7600; Hitachi Ltd, Tokyo, Japan). The size of the dispersed particles was extracted from the TEM image using image processing and analysis software (ImageJ 1.41n; National Institutes of Health, Bethesda, MD, USA). The hydrodynamic size and surface charge of the ZnO dispersions in solution were measured using DLS (Scatteroscope I; Qudix, Inc., Seoul, South Korea) and a particle analyzer (Zetasizer Nano ZS;

**Table I** Coating materials used in this study

	Structure	Charge
Cit		Negative
Tris		Positive
PAA		Negative
PAH		Positive
PLL		Positive

**Abbreviations:** Cit, sodium citrate; Tris, tris(2-aminoethyl)amine; PAA, poly(acrylic acid); PAH, poly(allylamine hydrochloride); PLL, poly-L-lysine hydrochloride.

Malvern Instruments Inc, Southborough, MA, USA), respectively. To monitor the colloidal stability of ZnO suspensions in cell culture media (37°C, 5% CO<sub>2</sub>), the OD, at 371 nm, was monitored using a UV-Vis spectrometer (Optizen 2120UV; Mecasys Co. Ltd., Daejeon, Korea).

### Cell culture and ZnO NP exposure

HeLa cells were purchased from the Korea Biological Resource Center (Daejeon, Korea). HeLa cells were cultured in fresh DMEM medium (Life Technologies Corp) including 10% FBS and 1% penicillin-streptomycin (15140-122, Life Technologies Corp). Cells suspensions, prepared at a concentration of 10<sup>4</sup>–10<sup>5</sup> cells/mL were loaded in the 96-well plate. Freshly isolated HeLa cells were cultured in a plastic Cell culture flask (SPL Lifesciences Co. Ltd., Seoul, Korea). After seeding, cells were maintained at 37°C in a 5% CO<sub>2</sub> incubator for 36 hours. Then, the HeLa cells were treated with 0, 10, 20, 30, 40, 50, and 60 mg/L ZnO,

ZnO<sup>(PAA)</sup>, or ZnO<sup>(PLL)</sup> in DMEM media without FBS or with FBS for 24 hours.

### Cell viability assay

The cytotoxicity of ZnO NPs toward HeLa cells was determined using a conventional WST assay protocol, which is based on the ability of mitochondrial dehydrogenase in viable cells to release water-soluble tetrazolium salt (WST, WST-1 assay kit, EZ-Cytox, Daeillab, Seoul, Korea), changing from a soluble slight red tetrazolium salt to orange formazan.

After media suction, 10% WST solution in DMEM cell culture media was added to HeLa cells treated with ZnO NPs, and the mixture was incubated for 2 hours at 37°C in a 5% CO<sub>2</sub> incubator. The cell culture media and WST solution were moved to another 96-well plate, and the absorbances were measured, at a wavelength of 450 nm, using a microplate reader (Multiskan EX; Thermo Fisher Scientific Inc., Waltham, MA, USA).

## Results and discussion

### Physicochemical characteristics of uncoated ZnO NPs

TEM was used to obtain information on the core diameter distributions and morphologies of the ZnO NPs (Figure 1). The core diameter distributions were estimated from image analysis of 500–1,000 ZnO NPs in representative TEM images (Figure 1). Most of the particles examined by TEM had spherical morphologies, and the core diameter distributions were in good agreement with manufacturer specifications, with the exception of the ZnO<sup>AE20</sup> particles. In agreement with the manufacturer's specification, the core diameters of ZnO<sup>AA20</sup>, ZnO<sup>SM20</sup>, and ZnO<sup>AE100</sup> were measured as 22±7 nm, 20±9 nm, and 63±26 nm, respectively, while the ZnO<sup>AE20</sup> (with manufacturer's specification of 10–30 nm) was found to have much larger core diameter (57±25 nm) than that of the manufacturer's specification, which might have been due to errors in the process of manufacturing, labeling, etc.

The hydrodynamic diameter and zeta potential of the ZnO NPs were analyzed in DIW (pH 6.8), and the results are summarized in Figure 1 (see bottom). All of the ZnO NPs showed a hydrodynamic diameter of approximately 200 nm, which was much larger than their core diameters. The differences between the core and hydrodynamic diameter distributions indicated that there was significant aggregation

or agglomeration of ZnO NPs in the DIW. The measured zeta potentials, 23.3, 25.9, 22.6, and 19.6 mV (for ZnO<sup>AA20</sup>, ZnO<sup>AE20</sup>, ZnO<sup>SM20</sup>, and ZnO<sup>AE100</sup>, respectively) were similar to each other, which is also in reasonable agreement with the previously reported point of zero charge (PZC) for ZnO particles (PZC ≈9.0).<sup>20,21</sup> In DIW, all of the uncoated and agglomerated ZnO particles were observed to sediment within 24 hours. For electrostatic stabilization of NPs, it has been previously reported that the absolute value of the zeta potential must be less than 30 mV even in solutions with low ionic strength.<sup>14,22</sup> Thus, the observed sedimentation of uncoated ZnO NPs in the DIW can be ascribed to the insufficient surface charges of ZnO NPs in DIW.

### Physicochemical characteristics of surface-modified ZnO NPs

The general approach to prepare stable NP dispersions is to increase the repulsive forces between particles, such as the steric and electrostatic forces.<sup>14</sup> A simple method typically used for stabilization of NPs is to incrementally change the electrostatic repulsive forces, via adjustment of the pH, to increase/decrease the NP surface charge and increase/decrease the repulsive force between particles; however, toxicity test media are quite limited in the control of solution. Another method used for stabilization of NPs is surface modification,

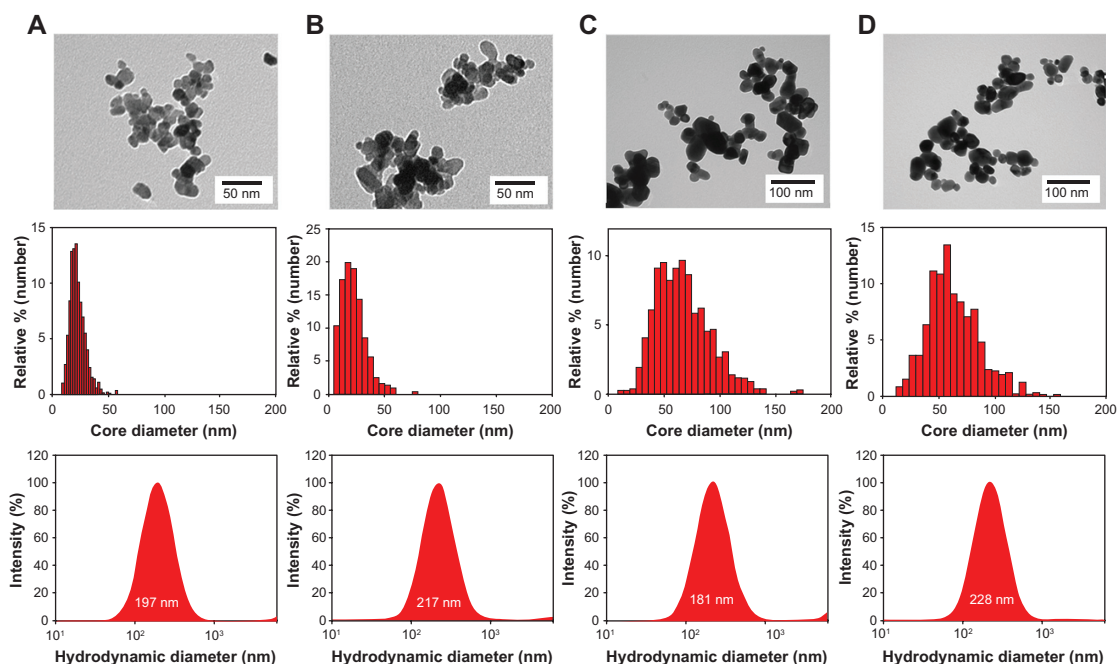


**Figure 1** Physicochemical characteristics of four commercial ZnO NPs in deionized water: (A) ZnO<sup>AA20</sup>, (B) ZnO<sup>SM20</sup>, (C) ZnO<sup>AE20</sup>, and (D) ZnO<sup>AE100</sup>.

**Notes:** The top row shows TEM images; the middle row shows core diameter distribution from TEM images; the bottom row shows hydrodynamic diameter from DLS.

**Abbreviations:** DLS, dynamic light scattering; TEM, transmission electron microscopy; NP, nanoparticle; ZnO<sup>AA20</sup>, 20 nm ZnO; ZnO<sup>AE20</sup>, 10–30 nm ZnO; ZnO<sup>AE100</sup>, <100 nm ZnO; ZnO<sup>SM20</sup>, 10–35 nm ZnO.

**Table 2** Hydrodynamic diameters and zeta potentials of different surface-coated ZnO<sup>AA20</sup> NPs in deionized water

	ZnO <sup>AA20</sup> (Cit)	ZnO <sup>AA20</sup> (Tris)	ZnO <sup>AA20</sup> (PAA)	ZnO <sup>AA20</sup> (PAH)	ZnO <sup>AA20</sup> (PLL)
Hydrodynamic diameter (nm)	317±10	421±47	198±37	208±10	237±31
Zeta potential (mV)	-35.2±1.6	22.6±2.1	-32.1±2.0	52.0±2.8	39.8±3.5

**Note:** The hydrodynamic diameter and zeta potential show results of average and standard deviation by three repetition in deionized water (about pH 7.0).

**Abbreviations:** NP, nanoparticle; ZnO<sup>AA20</sup>, 20 nm ZnO; ZnO<sup>AA20</sup>(Cit), sodium citrate-coated ZnO<sup>AA20</sup>; ZnO<sup>AA20</sup>(PAA), poly(acrylic acid)-coated ZnO<sup>AA20</sup>; ZnO<sup>AA20</sup>(PAH), poly(allyamine hydrochloride)-coated ZnO<sup>AA20</sup>; ZnO<sup>AA20</sup>(PLL), poly-L-lysine hydrochloride-coated ZnO<sup>AA20</sup>; ZnO<sup>AA20</sup>(Tris), tris(2-aminoethyl)amine-coated ZnO<sup>AA20</sup>.

using various types of ligands, which can control both steric and electrostatic forces between NPs. In this study, five different ligands were used for stabilization of the ZnO NPs.

The surfaces of ZnO<sup>AA20</sup> NPs were modified with the five different compounds listed in Table 1, and their hydrodynamic diameter and zeta potential in DIW are provided in Table 2. The surface charges were measured to be -35.2±1.6 mV for ZnO<sup>AA20</sup>(Cit), -32.1±2.0 mV for ZnO<sup>AA20</sup>(PAA), 22.6±2.1 mV for ZnO<sup>AA20</sup>(Tris), 52.0±2.8 mV for ZnO<sup>AA20</sup>(PAH), and 39.8±3.5 mV for the ZnO<sup>AA20</sup>(PLL) NPs, in DIW. The hydrodynamic diameters for the polymer ligand-coated ZnO NPs (ie, ZnO<sup>AA20</sup>(PAA), ZnO<sup>AA20</sup>(PAH), and ZnO<sup>AA20</sup>(PLL)) were measured to be approximately 200 nm, while the monomer ligand-coated ZnO NPs (ie, ZnO<sup>AA20</sup>(Cit) and ZnO<sup>AA20</sup>(Tris)) had larger sizes, of 317±10 and 421±47 nm, respectively. Polymer ligands contributed to the stabilization of NPs via steric and electrostatic forces, also referred to as electrosteric forces, while monomeric ligands contributed to the stabilization only through electrostatic repulsive forces. Thus, the polymer-coated ZnO NPs produced more stable suspensions than did the monomeric ligand-coated ZnO NPs. Our goal was the preparation of stable NPs in two in vitro toxicity test solutions (ie, RPMI and DMEM), which have a high ionic strength; 152 mM for RPMI and 169 mM for DMEM;<sup>23</sup> however, electrostatic stabilization of NPs via adsorption of small monomeric ligands is known to only be efficient at low ionic strengths (less than approximately 0.1 M).<sup>14</sup> Therefore, for

the study of colloidal stability in the in vitro toxicity test solution, we used two types of coating material – negatively charged PAA and positively charged PLL – for electrosteric stabilization. PAH was not used in this colloidal stability study, since PAH was found to be highly toxic to HeLa cells (data not shown).

## Colloidal stability of surface-modified ZnO NPs in cytotoxicity test media

The state of agglomeration and the extent of sedimentation play important roles in delivered dosimetry, cellular uptake, and the resultant cytotoxic effects of NPs in biological systems.<sup>15,24</sup> Therefore, for reliable and reproducible assessment of the potential toxicity of NPs on cellular systems, it is imperative to maintain the state of agglomeration and the extent of sedimentation in the actual cell culture media during the toxicity testing period. The ZnO<sup>AE20</sup> particles were not used in this colloidal stability study since there was a disagreement between the core sizes of our own measurements and those of the manufacturer. The other three ZnO NPs (ie, ZnO<sup>AA20</sup>, ZnO<sup>SM20</sup>, and ZnO<sup>AE100</sup>) were used for the colloidal stability study. Figure 2 and Figure 3 show the temporal variations of OD for the various ZnO NPs in RPMI and DMEM media without/with 10% FBS. Since the OD measured at 371 nm is linearly proportional to the amount of dispersed ZnO particles unless interfered with by scattering from heavily aggregated NPs, the optical

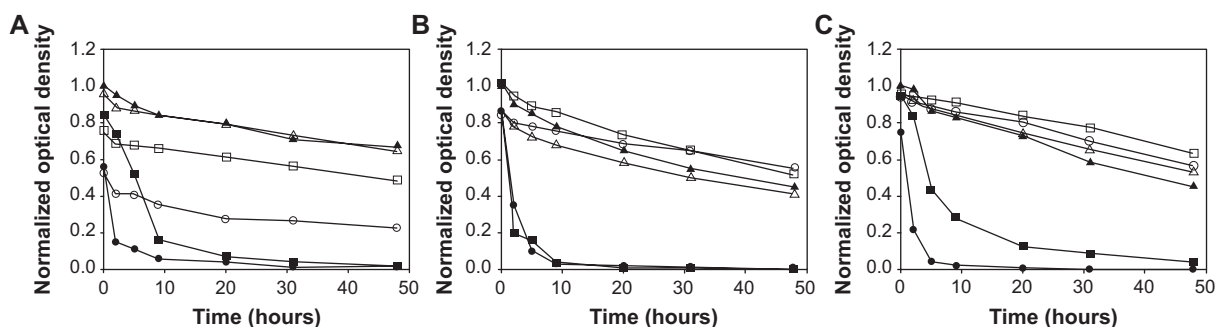


**Figure 2** Temporal variations in the optical density of ZnO dispersions in RPMI cell culture media: (A) ZnO<sup>AA20</sup>, (B) ZnO<sup>SM20</sup>, and (C) ZnO<sup>AE100</sup>.

**Notes:** Filled circles show uncoated ZnO without FBS; hollow circles show uncoated ZnO with FBS; filled triangles show PAA-coated ZnO without FBS; hollow triangles show PAA-coated ZnO with FBS; filled squares show PLL-coated ZnO without FBS; and hollow squares show PLL-coated ZnO with FBS.

**Abbreviations:** FBS, fetal bovine serum; PAA, poly(acrylic acid); PLL, poly-L-lysine hydrochloride; RPMI, Roswell Park Memorial Institute; ZnO<sup>AA20</sup>, 20 nm ZnO; ZnO<sup>AE100</sup>, <100 nm ZnO; ZnO<sup>SM20</sup>, 10–35 nm ZnO.



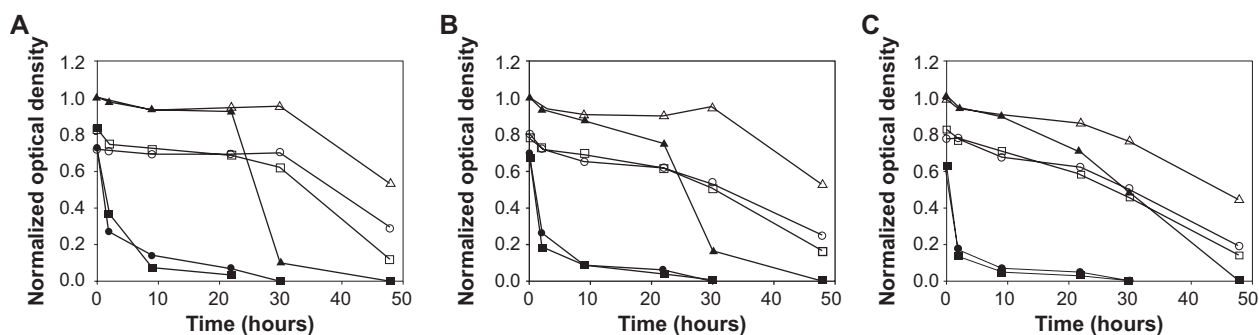


**Figure 3** Temporal variations in the optical density of ZnO dispersions in DMEM cell culture media: (A) ZnO<sup>AA20</sup>, (B) ZnO<sup>SM20</sup>, and (C) ZnO<sup>AE100</sup>.

**Notes:** Filled circles show uncoated ZnO without FBS; hollow circles show uncoated ZnO with FBS; filled triangles show PAA-coated ZnO without FBS; hollow triangles show PAA-coated ZnO with FBS; filled squares show PLL-coated ZnO without FBS; and hollow squares show PLL-coated ZnO with FBS.

**Abbreviations:** DMEM, Dulbecco's Modified Eagle's Medium; FBS, fetal bovine serum; PAA, poly(acrylic acid); PLL, poly-L-lysine hydrochloride; ZnO<sup>AA20</sup>, 20 nm ZnO; ZnO<sup>AE100</sup>, <100 nm ZnO; ZnO<sup>SM20</sup>, 10–35 nm ZnO.

density at 371 nm was used to monitor the degree of ZnO sedimentation.

In RPMI media without FBS (Figure 2A), rapid agglomeration and sedimentation of uncoated ZnO<sup>AA20</sup> were observed within a few hours. As mentioned earlier, the positively charged (19–25 mV) uncoated ZnO<sup>AA20</sup> NPs did not have enough surface charge to maintain a stable dispersion. The positively charged ZnO<sup>AA20(PLL)</sup> NPs were found to have a similar behavior to the uncoated ZnO<sup>AA20</sup> NPs, but the negatively charged ZnO<sup>AA20(PAA)</sup> NPs were found to be more resistant to agglomeration and sedimentation in the media, regardless of the primary size. These differences reflect the strength of adsorption between the surface of NPs and the polymer ligand. The positively charged surface amine groups (PLL) were weakly adsorbed onto the positive surface of ZnO, but the negatively charged surface carboxyl groups (PAA) seem to have stronger interactions with the ZnO surfaces.

FBS is generally added to *in vitro* toxicity media for cell growth, thus the effect of FBS on the stability of NPs is highly relevant to evaluation of the toxicity potential of NPs. For the effect of protein, it has been reported that the presence of FBS, bovine serum albumin (BSA), and

human serum albumin (HSA) in media notably enhanced the stability of NPs.<sup>18,19,25</sup> This stabilization occurs through electrosteric force, which can generally be achieved by attaching biomacromolecules to the surface of NPs.<sup>15</sup> In Figures 2A, 2B, and 2C, uncoated ZnO<sup>AA20</sup> and ZnO<sup>AA20(PLL)</sup> NPs were observed to give rapid sedimentation in the absence of FBS, whereas in the presence of FBS, these particles were better dispersed than the uncoated ZnO<sup>AA20</sup> NPs. This result shows that ZnO NPs are stable in suspension in the presence of FBS, which is in accordance with a previous study, by Allouni et al on the stability of TiO<sub>2</sub> NPs in RPMI containing FBS.<sup>18</sup> On the other hand, ZnO<sup>AA20(PAA)</sup> NPs were maintained in dispersion at 50%, regardless of the presence of FBS in RPMI media, and the hydrodynamic size distributions of the suspended particles were maintained in the range of 180–370 nm (Figure 4).

To examine the effect of the toxicity test medium, we prepared ZnO NPs in RPMI and DMEM media. As shown in Figures 2A, 2B, and 2C, when exposed to RPMI with FBS, the ZnO (ie, uncoated ZnO<sup>AA20</sup>, ZnO<sup>AA20(PAA)</sup>, and ZnO<sup>AA20(PLL)</sup>) NPs showed slow sedimentation over 48 hours, while rapid sedimentation of ZnO in DMEM with FBS was

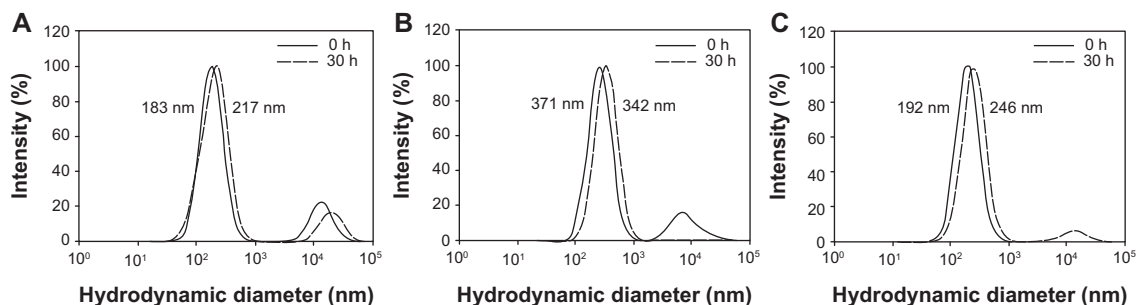


**Figure 4** Hydrodynamic diameter distributions of (A) ZnO<sup>AA20(PAA)</sup>, (B) ZnO<sup>SM20(PAA)</sup>, and (C) ZnO<sup>AE100(PAA)</sup>, after 0- and 30-hour exposures to RPMI media containing FBS.

**Abbreviations:** FBS, fetal bovine serum; h, hours; PAA, poly(acrylic acid); RPMI, Roswell Park Memorial Institute; ZnO<sup>AA20(PAA)</sup>, PAA-coated, 20 nm ZnO; ZnO<sup>AE100(PAA)</sup>, PAA-coated, <100 nm ZnO; ZnO<sup>SM20(PAA)</sup>, PAA-coated, 10–35 nm ZnO.

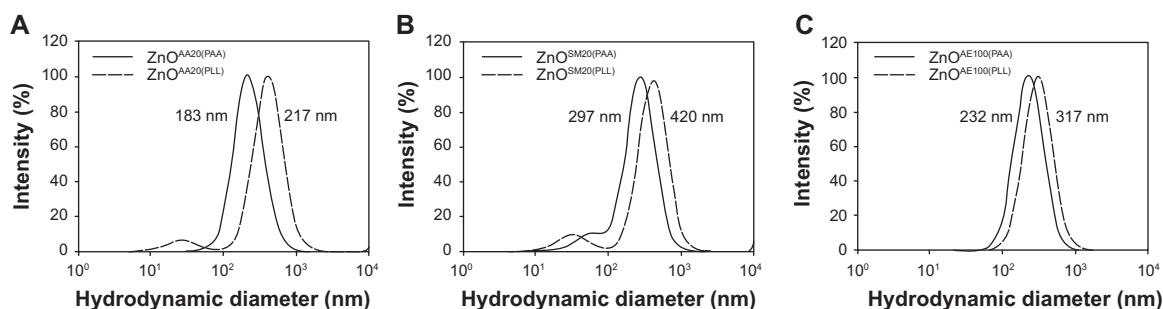


**Figure 5** Hydrodynamic diameter distributions of (A) ZnO<sup>AA20(PAA)</sup> and ZnO<sup>AA20(PLL)</sup>, (B) ZnO<sup>SM20(PAA)</sup> and ZnO<sup>SM20(PLL)</sup>, and (C) ZnO<sup>AE100(PAA)</sup> and ZnO<sup>AE100(PLL)</sup>, after 30-hour exposures to DMEM media containing FBS.

**Abbreviations:** FBS, fetal bovine serum, DMEM, Dulbecco's Modified Eagle's Medium; PAA, poly(acrylic acid); PLL, poly-L-lysine hydrochloride; ZnO<sup>AA20(PAA)</sup>, PAA-coated, 20 nm ZnO; ZnO<sup>AA20(PLL)</sup>, PLL-coated, 20 nm ZnO; ZnO<sup>AE100(PAA)</sup>, PAA-coated, <100 nm ZnO; ZnO<sup>AE100(PLL)</sup>, PLL-coated, <100 nm ZnO; ZnO<sup>SM20(PAA)</sup>, PAA-coated, 10–35 nm ZnO; ZnO<sup>SM20(PLL)</sup>, PLL-coated, 10–35 nm ZnO.

observed after 24 hours (Figure 3A–C), and the hydrodynamic size distributions of suspended particles were maintained in the range of 200–420 nm (Figure 5). Similar results were seen in our previous studies,<sup>15</sup> in which 70 nm TiO<sub>2</sub> NPs were more dispersed in RPMI than in DMEM media with FBS. These observations indicate that physicochemical properties of the media, such as higher ionic strength (169 mM for DMEM versus 152 mM for RPMI) and greater quantity of inorganic components (in DMEM),<sup>23</sup> may be responsible for the differences in NP stability. Additionally, differences in the organic components of the media play key roles in determining the colloidal stability of NPs in aqueous environments.

## Cell viability of surface-modified ZnO NPs

Cell viability assays were also performed to observe the effects of surface-modifying ligands and charges on the cytotoxicity of ZnO NPs. HeLa cells were exposed to 0–60 mg/L of uncoated ZnO<sup>AA20</sup>, ZnO<sup>AA20(PAA)</sup>, and ZnO<sup>AA20(PLL)</sup> NPs for 24 hours. Interestingly, surface charge-dependent trends in ZnO cytotoxicity were observed for those cells exposed in DMEM media without FBS. The positively charged ZnO NPs (ZnO<sup>AA20(PLL)</sup>) were found slightly more toxic than the other two NPs (ZnO<sup>AA20</sup> and ZnO<sup>AA20(PAA)</sup>) (with 50% lethal concentration [LC<sub>50</sub>] values of 21.7 mg/L, 20.5 mg/L, and 17.9 mg/L for the ZnO<sup>AA20</sup>, ZnO<sup>AA20(PAA)</sup>, and ZnO<sup>AA20(PLL)</sup> NPs, respectively). Our observations that ZnO<sup>AA20(PLL)</sup> NPs were more toxic than ZnO<sup>AA20(PAA)</sup> in the absence of FBS is in good agreement with the literature.<sup>26,27</sup> Previously, it was also reported that cellular NP association is closely related to the surface charge of NPs.<sup>28,29</sup> Slowing et al<sup>29</sup> confirmed that positively charged SiO<sub>2</sub> NPs (12.8 mV) were preferred for cellular association compared with negatively charged

SiO<sub>2</sub> NPs (–34.7 mV), while Ali-Boucetta et al also reported that A549 cells preferred to associate with MWCNT-NH<sub>3</sub><sup>+</sup> than with negatively charged MWCNT.<sup>28</sup> Therefore, the surface charge-dependent toxicity of ZnO NPs can be ascribed to the electrostatic interactions between the cell membranes and NPs, where the negatively charged HeLa cell membranes exhibit attractive forces with positively charged ZnO NPs and repulsive forces with negatively charged ZnO NPs.<sup>30</sup>

However, these surface charge-dependent trends in ZnO cytotoxicity were not observed for those cells cultured in FBS-containing DMEM media. In the presence of FBS, the cytotoxicities of ZnO NPs were significantly reduced and found similar to each other (LC<sub>50</sub> values of 24.4 mg/L, 24.8 mg/L, and 24.2 mg/L for the ZnO<sup>AA20</sup>, ZnO<sup>AA20(PAA)</sup>, and ZnO<sup>AA20(PLL)</sup> NPs, respectively), despite of their differences in surface-modifying ligands and charges. Optical images, shown in Figure 6, also confirmed these reduced cytotoxicities in the presence of FBS. The HeLa cells exposed to ZnO NPs in the presence of FBS were found mostly healthy and well attached on the cell culture plates, while those exposed to ZnO NPs in the absence of FBS displayed shrinkage and rounding of cellular shapes, which are typical morphological changes observed in cell death processes.<sup>31</sup> These observations can be ascribed to the formation of “protein corona” on the surfaces of the ZnO NPs. According to recent studies,<sup>32–35</sup> the “surfaces” of NPs in biological media (eg, blood plasma) were often modified by the adsorption of biomolecules (eg, proteins), leading to a formation of a NP–biomolecular interface. In particular, the NP–protein interfaces were named as “protein corona” and further divided into “hard” and “soft” coronas, depending on their exchange rates at the surface of NPs. Additionally, the enhancements of ZnO colloidal stability (Figure 3) in the

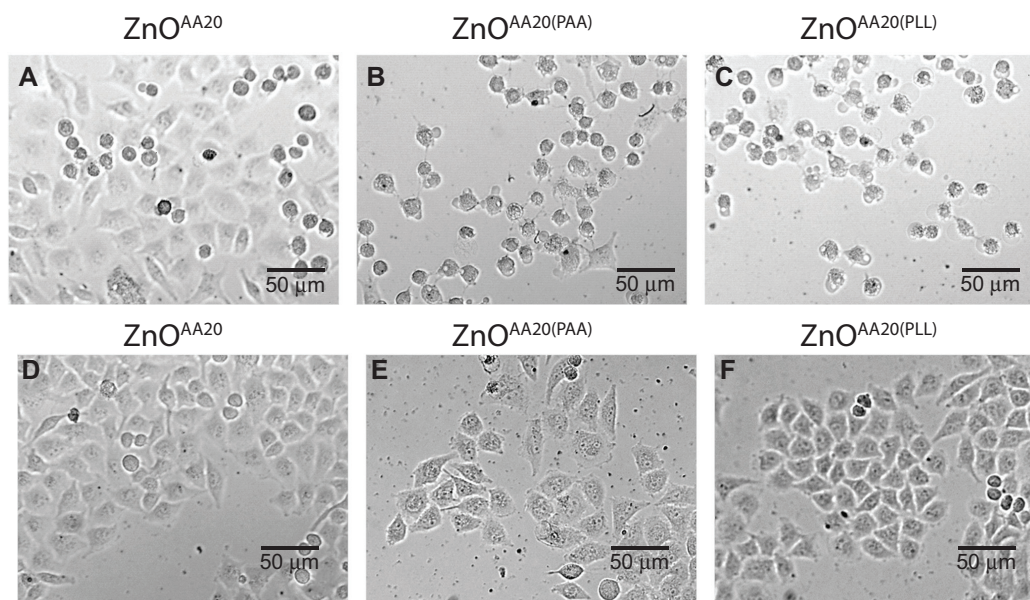


**Figure 6** Optical images of HeLa cells exposed to (A) ZnO<sup>AA20</sup>, (B) ZnO<sup>AA20(PAA)</sup>, and (C) ZnO<sup>AA20(PLL)</sup>, in DMEM without FBS; and (D) ZnO<sup>AA20</sup>, (E) ZnO<sup>AA20(PAA)</sup>, and (F) ZnO<sup>AA20(PLL)</sup>, in DMEM with FBS.

**Notes:** Exposed concentration of ZnO; 20 mg/L.

**Abbreviations:** FBS, fetal bovine serum; DMEM, Dulbecco's Modified Eagle's Medium; ZnO<sup>AA20</sup>, 20 nm ZnO; ZnO<sup>AA20(PAA)</sup>, poly(acrylic acid)-coated, 20 nm ZnO; ZnO<sup>AA20(PLL)</sup>, poly-L-lysine hydrochloride-coated, 20 nm ZnO.

presence of FBS may also have contributed to the reduced cytotoxicity of the ZnO NPs. Due to electrosteric interactions between the ZnO NP–protein interfaces, the ZnO NPs were found much more stable in DMEM cell culture media in the presence of FBS. These enhancements in colloidal stability are expected to reduce the delivered dose of ZnO NPs by minimizing the agglomeration and sedimentation of NPs. We think that in the presence of FBS, the interactions between the ZnO NPs and the biomolecules overwhelmed the effects of primary surface-modifying ligands and induced much lower cytotoxicities, independently of their primary surface-modifying ligands. These results confirmed the importance of surface-modifying ligands and charges on the resultant toxicities of NPs. Moreover, in addition to the primary surface-modifying ligands, the biomolecules present in cell culture media or blood plasma will also play a key role in determining the cytotoxicity of NPs, via secondary modification of the NP surface (eg, protein corona).

## Conclusion

In order to evaluate the effects of extrinsic physicochemical properties on the cytotoxicity of NPs, we performed a set of physicochemical characterizations and simple cell viability assays of commercially available ZnO NPs. Our results showed that polymer-coated ZnO NPs with highly negative and/or positive surface charges were better dispersed in toxicity test media. In FBS-free media, ZnO NPs were found to

be highly agglomerated and sedimented within a few hours, whereas the presence of FBS in the toxicity test media notably enhanced the stability of ZnO NP suspensions for a period of 48 hours. For the HeLa cells exposed to ZnO NPs in FBS-free DMEM media, surface charge-dependent cytotoxicity trends were observed. However, these trends were not observed for those cells cultured in FBS-containing DMEM media, which confirmed the important roles of surface-modifying ligands (eg, primary surface-modifying ligands as well as the protein corona from biological media) on the resultant cytotoxicities of NPs.

## Acknowledgments

This research was supported by a grant (number 10182MFDS991) from the Ministry of Food and Drug Safety in 2010–2013.

## Disclosure

The authors report no conflicts of interest in this work.

## References

- Osmond MJ, McCall MJ. Zinc oxide nanoparticles in modern sunscreens: an analysis of potential exposure and hazard. *Nanotoxicology*. 2010;4(1):15–41.
- Chaudhry Q, Scotter M, Blackburn J, et al. Applications and implications of nanotechnologies for the food sector. *Food Addit Contam Part A Chem Anal Control Expo Risk Assess*. 2008;25(3):241–258.
- Deng X, Luan Q, Chen W, et al. Nanosized zinc oxide particles induce neural stem cell apoptosis. *Nanotechnology*. 2009;20(11):115101.



4. Adams LK, Lyon DY, Alvarez PJ. Comparative eco-toxicity of nanoscale TiO<sub>2</sub>, SiO<sub>2</sub>, and ZnO water suspensions. *Water Res.* 2006; 40(19):3527–3532.
5. Brayner R, Ferrari-Iliou R, Brivois N, Djediat S, Benedetti MF, Fiévet F. Toxicological impact studies based on Escherichia coli bacteria in ultrafine ZnO nanoparticles colloidal medium. *Nano Lett.* 2006;6(4):866–870.
6. Zhang L, Jiang Y, Ding Y, Povey M, York D. Investigation into the antibacterial behaviour of suspensions of ZnO nanoparticles (ZnO nanofluids). *J Nanopart Res.* 2007;9(3):479–489.
7. Auffan M, Rose J, Bottero JY, Lowry GV, Jolivet JP, Wiesner MR. Towards a definition of inorganic nanoparticles from an environmental, health and safety perspective. *Nat Nanotechnol.* 2009;4(10):634–641.
8. Nel A, Xia T, Madler L, Li N. Toxic potential of materials at the nanolevel. *Science.* 2006;311(5761):622–627.
9. Powers KW, Brown SC, Krishna VB, Wasdo SC, Moudgil BM, Roberts SM. Research strategies for safety evaluation of nanomaterials. Part VI. Characterization of nanoscale particles for toxicological evaluation. *Toxicol Sci.* 2006;90(2):296–303.
10. Kwon DW, Jeon SK, Yoon TH. Impact of agglomeration on the bioaccumulation of sub-100 nm sized TiO<sub>2</sub>. *Colloids Surf B Biointerfaces.* 2014;116:277–283.
11. Hsiao IL, Huang YJ. Effects of various physicochemical characteristics on the toxicities of ZnO and TiO nanoparticles toward human lung epithelial cells. *Sci Total Environ.* 2011;409(7):1219–1228.
12. Peng X, Palma S, Fisher NS, Wong SS. Effect of morphology of ZnO nanostructures on their toxicity to marine algae. *Aquat Toxicol.* 2011;102(3–4):186–196.
13. Jiang W, Mashayekhi H, Xing B. Bacterial toxicity comparison between nano- and micro-scaled oxide particles. *Environ Pollut.* 2009;157(5):1619–1625.
14. Jiang J, Oberdörster G, Biswas P. Characterization of size, surface charge, and agglomeration state of nanoparticle dispersions for toxicological studies. *J Nanopart Res.* 2009;11(1):77–89.
15. Lee SH, Kwon D, Yoon TH. An optimized dispersion of manufactured nanomaterials for in vitro cytotoxicity assays. *Toxicol Environ Health Sci.* 2010;2(3):207–213.
16. Murdock RC, Braydich-Stolle L, Schrand AM, Schlager JJ, Hussain SM. Characterization of nanomaterial dispersion in solution prior to in vitro exposure using dynamic light scattering technique. *Toxicol Sci.* 2008;101(2):239–253.
17. Meibner T, Potthoff A, Richter V. Suspension characterization as important key for toxicological investigations. *Journal of Physics Conference Series.* 2009;170(1):012012.
18. Allouni ZE, Cimpan MR, Høl PJ, Skodvin T, Gjerdet NR. Agglomeration and sedimentation of TiO<sub>2</sub> nanoparticles in cell culture medium. *Colloids Surf B Biointerfaces.* 2009;68(1):83–87.
19. Bihari P, Vippola M, Schultes S, et al. Optimized dispersion of nanoparticles for biological in vitro and in vivo studies. *Part Fibre Toxicol.* 2008;5:14.
20. Yatmaz HC, Akyol A, Bayramoglu M. Kinetics of the photocatalytic decolorization of an azo reactive dye in aqueous ZnO Suspensions. *Ind Eng Chem Res.* 2004;43(19):6035–6039.
21. Kosmulski M. pH-dependent surface charging and points of zero charge II. Update. *J Colloid Interface Sci.* 2004;275(1):214–224.
22. International Organization for Standardization (ISO). *Sample Preparation – Dispersing Procedures for Powder in Liquids* [ISO 14887:2000]. Geneva: ISO; 2010.
23. Kwon D, Lee SH, Kim J, Yoon TH. Dispersion, fractionation and characterization of sub-100 nm P25 TiO<sub>2</sub> nanoparticles in aqueous media. *Toxicol Environ Health Sci.* 2010;2(1):78–85.
24. Yoon D, Woo D, Kim JH, et al. Agglomeration, sedimentation, and cellular toxicity of alumina nanoparticles in cell culture medium. *J Nanopart Res.* 2011;13(6):2543–2551.
25. Liu W, Zhou QF, Liu JY, Fu JJ, Liu SJ, Jiang GB. Environmental and biological influences on the stability of silver nanoparticles. *Chinese Science Bulletin.* 2011;56:2009–2015.
26. Arvizo RR, Miranda OR, Thompson MA, et al. Effect of nanoparticle surface charge at the plasma membrane and beyond. *Nano Lett.* 2010;10(7):2543–2548.
27. Asati A, Santra S, Kaittanis C, Perez JM. Surface-charge-dependent cell localization and cytotoxicity of cerium oxide nanoparticles. *ACS Nano.* 2010;4(9):5321–5331.
28. Ali-Boucetta H, Al-Jamal KT, Müller KH, et al. Cellular uptake and cytotoxic impact of chemically functionalized and polymer-coated carbon nanotubes. *Small.* 2011;7(22):3230–3238.
29. Slowing I, Trewyn BG, Lin VS. Effect of surface functionalization of MCM-41-type mesoporous silica nanoparticles on the endocytosis by human cancer cells. *J Am Chem Soc.* 2006;128(46):14792–14793.
30. Yoo HJ, Yoon TH. Flow cytometric assessment of ROS generations that are directly related to cellular ZnO nanoparticle uptake. *J Nanosci Nanotechnol.* 2014;14(7):5395–5401.
31. Kim MJ, Lim KH, Yoo HJ, Rhee SW, Yoon TH. Morphology-based assessment of Cd<sup>2+</sup> cytotoxicity using microfluidic image cytometry (microFIC). *Lab Chip.* 2010;10(4):415–417.
32. Dobrovolskaia MA, Patri AK, Zheng J, et al. Interaction of colloidal gold nanoparticles with human blood: effects on particle size and analysis of plasma protein binding profiles. *Nanomedicine.* 2009;5(2):106–117.
33. Lundqvist M, Stigler J, Elia G, Lynch I, Cedervall T, Dawson KA. Nanoparticle size and surface properties determine the protein corona with possible implications for biological impacts. *Proc Natl Acad Sci U S A.* 2008;105(38):14265–14270.
34. Cedervall T, Lynch I, Lindman S, et al. Understanding the nanoparticle-protein corona using methods to quantify exchange rates and affinities of proteins for nanoparticles. *Proc Natl Acad Sci U S A.* 2007;104(7):2050–2055.
35. Walczyk D, Bombelli FB, Monopoli MP, Lynch I, Dawson KA. What the cell “sees” in bionanoscience. *J Am Chem Soc.* 2010; 132(16):5761–5768.

## International Journal of Nanomedicine

### Publish your work in this journal

The International Journal of Nanomedicine is an international, peer-reviewed journal focusing on the application of nanotechnology in diagnostics, therapeutics, and drug delivery systems throughout the biomedical field. This journal is indexed on PubMed Central, MedLine, CAS, SciSearch®, Current Contents®/Clinical Medicine,

Submit your manuscript here: <http://www.dovepress.com/international-journal-of-nanomedicine-journal>

Dovepress

Journal Citation Reports/Science Edition, EMBase, Scopus and the Elsevier Bibliographic databases. The manuscript management system is completely online and includes a very quick and fair peer-review system, which is all easy to use. Visit <http://www.dovepress.com/testimonials.php> to read real quotes from published authors.